



Article

Critical Influences of Plasma pH on Human Protein Properties for Modeling Considerations: Size, Charge, Conformation, Hydrophobicity, and Denaturation

Majak Mapiour¹ and Abdelrasoul Amira^{1,2,*} 

¹ Department of Chemical and Biological Engineering, College of Engineering, University of Saskatchewan, 57 Campus Drive, Saskatoon, SK S7N 5A9, Canada

² Division of Biomedical Engineering, College of Engineering, University of Saskatchewan, 57 Campus Drive, Saskatoon, SK S7N 5A9, Canada

* Correspondence: amira.abdelrasoul@usask.ca; Tel.: +1-(306)-966-2946; Fax: +1-(306)-966-4777

Abstract: The fouling of biomaterials (e.g., membranes) by plasma proteins has always garnered attention because it renders biomedical devices ineffective and can jeopardize the patient's well-being. Modeling the fouling process sheds light on its mechanisms and helps improve the biocompatibility of biomaterials. Assuming proteins to be hard spheres with uniform surface properties reduces the modeling complexity, but it seriously deviates from the accurate, real perspective. One reason for the inaccuracy is that proteins' properties tend to change as environmental factors such as pH and ionic strength are varied. This study critically reviews the pH-induced changes in protein properties, namely size, charge, conformity, hydrophobicity, and denaturation. Though these properties may be interrelated, they are addressed individually to allow for a thorough discussion. The study illustrates the necessity of incorporating the protein property changes resulting from pH alteration to better explain and model the fouling process. The discussion is focused on human serum albumin and fibrinogen. Human serum albumin is the most abundant plasma protein, while fibrinogen plays a major role in blood clotting and triggering of the thrombogenic response.

Keywords: protein properties; albumin; fibrinogen; pH; conformation; protein structure



Citation: Mapiour, M.; Amira, A. Critical Influences of Plasma pH on Human Protein Properties for Modeling Considerations: Size, Charge, Conformation, Hydrophobicity, and Denaturation. *J. Compos. Sci.* **2023**, *7*, 28. <https://doi.org/10.3390/jcs7010028>

Academic Editor:
Francesco Tornabene

Received: 19 November 2022

Revised: 10 December 2022

Accepted: 3 January 2023

Published: 10 January 2023



Copyright: © 2023 by the authors. Licensee MDPI, Basel, Switzerland. This article is an open access article distributed under the terms and conditions of the Creative Commons Attribution (CC BY) license (<https://creativecommons.org/licenses/by/4.0/>).

1. Introduction

Plasma protein fouling of biomaterials is an area of concern since it can adversely affect the performance of biomedical devices such as membranes in hemodialysis and hemoconcentration dialyzers. Fouling may lead to serious device malfunctioning during a treatment and result in the patient experiencing life-threatening complications [1]. Modeling the fouling process is one of the approaches researchers have been using to better understand fouling mechanisms and optimize the biocompatibility and performance of biomaterials.

To simplify the modeling process, proteins are often assumed to be hard spheres [2]. However, it is well known that protein properties, and thus protein interactions, are affected by environmental factors such as blood pH and ionic strength. In a recent study, Stradner and Schurtenberger [3] argued that developing improved models to describe protein behavior and interactions requires moving away from the hard-sphere view and towards considering proteins as patchy, responsive, and anisotropic particles. A study by Su et al. [4] clearly illustrated the responsiveness of a human serum protein to its environment. They observed internal and external fouling of ceramic ultrafiltration membranes (200 and 2000 Å) caused by human serum albumin (HSA) at pH values of 3, 5, and 7. Using Small-Angle Neutron Scattering (SANS), the authors concluded that at the pH of 3, the external fouling was more significant than the internal fouling, while at the pH of 5, the opposite was observed. The extent of internal fouling at pH 7 was found to be between that of the aforementioned

pH values. Such protein behavior changes are often attributed to alterations in the protein properties caused by environmental factors such as pH, which is the focus of this endeavor.

Frequently, the effects of ionic strength on protein properties are studied alongside those of pH. The main effect of increasing ionic strength is shielding the charge of the protein, resulting in a shorter Debye length and weakening the electrostatic repulsion forces [5]. Nattich-Rak et al. [6] reported that the absolute value of zeta potential of HSA decreases as the ionic strength is increased at all pH values accepted at HSA's isoelectric point. For example, at pH of 7.4, the HSA zeta potential values were about -20 , -29 , and -38 mV at ionic strength (NaCl) values of 0.15 M, 0.05 M, and 0.01 M, respectively. Similar effects of the ionic strength were reported by Tsapikouni and Missirlis [7] for fibrinogen.

Therefore, the goal of this critical review is to primarily investigate the influence of plasma pH on protein size, charge, hydrophobicity, conformation, and denaturation. This study focuses on how a protein may deviate from the hard-sphere view by examining the alterations in fibrinogen and human serum albumin properties as the pH is varied.

2. Human Serum Albumin (HSA) Structure

Human serum albumin (HSA), with a molecular mass of 66.5 kDa, accounts for over 50% of plasma proteins with a concentration in the range of 30–50 g/L. It is often the focus of many protein fouling studies in the biomedical field, since a foulant concentration is a key fouling factor. A closer look at HSA structure reveals its “patchy and anisotropic” nature. Its heart-shaped structure is a result of a single polypeptide forming a 3D structure composed of three similar domains, namely Domains I, II, and III. Each domain has subdomains A and B. HSA's polypeptide has 585 amino acids with residue 1–195, residue 196–383, and residue 384–585 forming Domains I, II, and III, respectively [8–10].

HSA is composed of hydrophilic and hydrophobic regions. Its overall hydropath value of -230.8 indicates hydrophilic properties. However, it also possesses pockets/cavities with strong hydrophobic properties [11,12]. Examples of such hydrophobic cavities are Sudlow site I and Sudlow site 2, which are in subdomains IIA and IIIA [13].

Though the three domains of HSA are structurally comparable, they differ in terms of amino acid sequences. Percentagewise, the similarities between domains 1 and 2, domains 1 and 3, and domains 2 and 3 are 25%, 18%, and 20%, respectively [14]. These differences among the domains result in non-homogenous distribution of hydrophobic patches and charges.

3. Human Serum Fibrinogen (FB) Structure

Fibrinogen adsorbs almost instantly when it contacts biomaterials. It then facilitates the adhesion of other blood components such as platelets and monocytes, further exacerbating fouling [15]. Additionally, fibrinogen adsorption can trigger thrombogenic and inflammatory responses [16]. The binding strength of fibrinogen to biomaterials is the highest among major plasma proteins, and it has considerable abundance in the range of 2–3 g/L [17]. For these reasons, fibrinogen is frequently the focus of study in protein fouling and biomaterial biocompatibility improvement research.

Fibrinogen's molecular mass is 340 kDa, and it consists of six polypeptide chains (two $A\alpha$, two $B\beta$, and two γ). The $A\alpha$, $B\beta$, and γ polypeptide chains are made up of 610, 461, and 411 amino acid residues, respectively [18]. The molecular mass of each chain is 66.5, 52, and 46.5 kDa, respectively [19]. The chains are held together by disulfide bonds, and they intertwine, forming a structure of globular regions which are connected. These regions are the E domain, two D domains, and two αC domains. The E domain contains the N-terminals of the all the polypeptide chains, whereas the D domains combine the C-terminals of the $B\beta$ and γ chains. The remaining C-terminals of the $A\alpha$ form the two αC domains [20,21]. The E domain is linked to the two D domains by α -helical coiled coils [22]. In comparison to the αC domains, the E and D domains are much more hydrophobic [23]. Furthermore, at physiological pH, the αC domains are positively charged while the E and D domains possess negative charges [24].

4. pH Effects on Human Serum Protein Properties

As mentioned earlier, the focus of this endeavor is to look at the effect of pH on the charge, size, hydrophobicity, and conformation of the HSA and fibrinogen. The subsequent sections tackle these topics. The selected properties may be interrelated, but for the sake of clarity, they are discussed separately.

4.1. Effect of pH of Protein Charge

The pH affects the charge of a protein by altering the protonation state charge-carrying amino acids, α -carboxyl, and α -amino terminal groups [25]. Generally, as pH increases, a protein's net charge changes from positive to negative, passing through zero at the isoelectric point [26].

4.1.1. Effect of pH on Albumin Charge

HSA possesses more negatively charged residues (98) than positively charged ones (83) [27]. The positive charges are due to amino acids such as arginine and lysine, while the negative charges are due to aspartic acid and glutamic acid [28]. Elsewhere, the negative and positive residues for HSA were reported to be 89 and 80, respectively [29]. At any rate, the negatively charged residues outnumber the positively charged residues. HSA has a charge of ~ 30 at pH of 4, 0 at the isoelectric point of 5.4, ~ -19 at pH of 7.4, and ~ -30 at pH of 9 [30].

HSA polypeptide contains 36 aspartic acids and 62 glutamic acids [31], and the pKa values of their carboxylic side chains are 3.9 and 4.2, respectively. These side chains are mostly protonated when the pH is less than their pKa, and thus are uncharged. As the pH is increased above their pKa, the carboxylic side chains of these amino acids are mostly deprotonated and become negatively charged. Conversely, arginine and lysine are mainly responsible for HSA acquiring positive charges. There are 24 arginine amino acids and 59 lysine amino acids in a HSA polypeptide [31]. The arginine and lysine side chains are a guanidinium group and an amino group which have pKa values of 12.5 and 10.8, respectively. They are positively charged at pH values below their pKa. Another rarely mentioned amino acid that may contribute to the positive charge of HSA is histidine. Perhaps due to the relatively lower pKa of 6, its contribution is considered minimal, and thus it is hardly mentioned in the literature. HSA possess 16 histidine amino acids [31].

Proteins' net charges are expressed in various ways, including electrophoretic mobility, effective charge, Debye–Huckel–Henry charge, and zeta potential. These quantities are related. Zeta potential can be obtained from the measured electrophoretic mobility via Smoluchowski's equation, as shown in Equation (1) (rearranged from [32]). The effective charge and the Debye–Huckel–Henry charge are also related to the electrophoretic mobility, as expressed in Equations (2) and (3), respectively [33]:

$$\zeta = \frac{3v_E\mu}{2\varepsilon_0\varepsilon_R(1 + \kappa r)} \quad (1)$$

where:

ζ = zeta potential;

v_E = electrophoretic mobility;

μ = solution viscosity;

ε_0 = vacuum permittivity;

ε_R = solvent dielectric constant;

r = particle radius;

κ = Debye–Huckel parameter.

$$Z_{DHH} = v_E(6\pi\mu r) \frac{1 + \kappa r}{f(\kappa r)} \quad (2)$$

where:

Z_{DHH} = Debye–Huckel–Henry charge;
 $f(\kappa r)$ = Henry correction factor.

$$Z_{Eff} = v_E(6\pi\mu r) \quad (3)$$

where:

Z_{Eff} = effective charge.

Generally, net charge characteristics of particles, macromolecules, and surfaces are often reported in terms of the zeta potential. Jun et al. [34] claimed that charge or electrostatic characteristics are better observed using zeta potential than surface charge. The relationship between the HSA zeta potential and pH has a reverse sigmoidal shape. In terms of modeling, this relationship can be expressed using a modified form of the Boltzmann sigmoidal equation.

Instead of focusing on the effect of pH on the net charge when modeling protein interactions (i.e., protein–protein or protein–surface interactions), Božič and Podgornik [26] argued that greater attention should be given to the distribution of charges in space (i.e., surface charge distribution) since this affects the orientation of protein interactions. The authors computed the surface charges of HSA at different pH values using canonical static dissociation constant pKa value of exposed amino acid residues. Calculations were carried out assuming HSA in monopole (i.e., net charge) and quadrupole moments. It was illustrated that in the monopole, the relationship between the charge and pH exhibited a reverse sigmoidal shape. However, in the quadrupole, the relationship depended on the spatial orientation of the protein. The authors commented that a better picture of the effect pH of a protein could be obtained by considering higher multiple moments but with added computational complexity.

4.1.2. Effect of pH on Fibrinogen Charge

The isoelectric point (pI) of fibrinogen is around 5.8; thus, it possesses a net negative charge (−7.6 to −8) at the physiological pH [35,36]. Though the net charge is negative at such a pH, the α C domains carry positive charges, while the D and E domains are negatively charged [20]. Fibrinogen's zeta potential vs. pH relationship also exhibits a reverse sigmoidal shape.

Kusova et al. [37] reported that under physiological conditions (pH = 7.4 and ionic strength = 0.15 M), the total charges of fibrinogen at the pH values of 3.5, 7.4, and 9.5 are +26, −8, and −18, respectively. Using these values, Adamczyk et al. [36] illustrated the anisotropic charge distribution of fibrinogen by computing the local charges of each domain (see Figure 1). For instance, at pH of 7.4, they determined the charges of the local charge of the E domain, D domains (two domains), and α -C domains (two domains) to be −6, −4, and +3, respectively. However, at pH < 4, the local charges of these domains were estimated to be +4, +6, and +5, respectively. The implication of this observation on conformation is discussed later. Furthermore, Wasilewska and Adamczyk [38] stated that the “patchy” nature of fibrinogen may explain its ability to adsorb to similarly charged surfaces. The authors expounded that although at a given pH, the zeta potentials of a protein and a surface may reveal that both entities possess strong negative charges, adsorption could still occur. As such, they argued against treating fibrinogen as a homogeneously charged particle but rather as a dipole.

4.2. Influence of pH on Human Serum Protein Conformation

4.2.1. Effect of pH on HSA Conformation

HSA manifests different conformational isomers as the pH is varied, as presented in Table 1. The isomerization process is reversible over a large pH range (2.7–10). The E-form (extended) is observed for pH below 2.7, and as the pH is increased to values between 2.7 and 4.3, HSA transitions to F-form (fast). A further increase in pH from 4.3 to 8 results in the N-form or the norm form, which is the common HSA conformation at physiological pH.

For pH ranges of 8 to 10 and 10 to 12, yet further conformational alternations occur, yielding the B-form (basic) and A-form (aged), respectively [39–42]. HSA expands and loses order as its conformation transitions from N to E as well as from N to A.

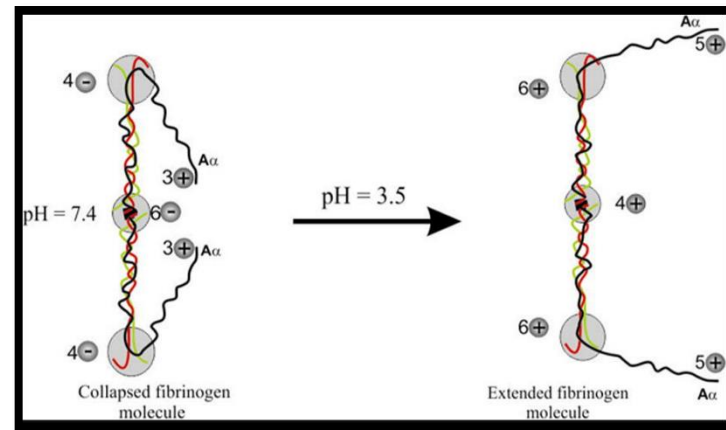


Figure 1. Effect of pH on fibrinogen charge distribution [36].

Table 1. HSA conformational transitions as the pH is varied [41,42].

Conformation Name	Conformation Alias	pH Range
Extended	E-Form	<2.7
Fast or fast migrating	F-Form	2.7–4.3
Norm	N-Form	4.3–8
Basic	B-Form	8–10
Aged	A-Form	10–12

The N-form of HSA is the dominant conformation within the physiological pH range; thus, researchers often find it to be of interest. Sønderby et al. [43] have shown that HSA in solution around the physiological pH is better described as an ellipsoid rather than a sphere. They stated that thermodynamic data accurately fit the ellipsoid model. The principal semi-axes (a, b, and c) of the ellipsoidal HSA were determined to be a = 4.14 nm, b = 3.27, and C = 2.77 nm [44].

4.2.2. Effect of pH on Fibrinogen Conformation

The E domain of the fibrinogen molecule is connected to the two peripheral D domains by sections of the intertwined $A\alpha$, $B\beta$, and γ (often referred to as coiled coils) [20]. The D domains are connected to the αC domains by a portion of $A\alpha$ (see Figure 2). As mentioned earlier, at a pH value around the physiological pH, the αC domains (positive) and the E domain (negative) carry opposite charges. Consequently, they attract each other, and thus the parts of $A\alpha$ that connect them fold towards the main body of the molecules, forming a compacted structure. For acidic (<4) and basic (>8) pH values, these $A\alpha$ arms extend away from the main body of the molecules due the similarity of charges between the E domain and the αC domains, resulting in an extended shape [24]. The charges are negative for acidic pH values and positive under basic conditions [35].

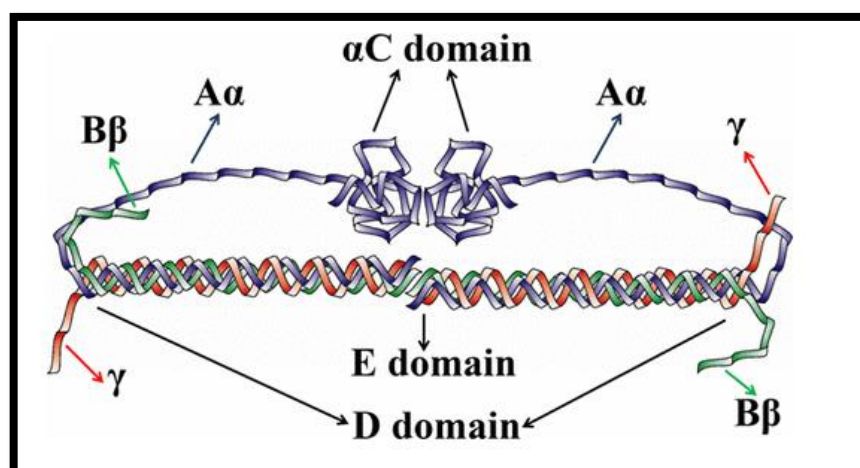


Figure 2. Fibrinogen structure [20].

By estimating the charge distribution of a fibrinogen molecule under physiological, acidic, and basic pH values, Adamczyk et al. [36] predicted the angles between the $A\alpha$ and the main body of a fibrinogen molecule. The angles were 56° at pH of 7.4 and 115° at $pH < 4$ and $pH > 10$. These angles highlight that fibrinogen has a compact conformation at neutral pH; however, the $A\alpha$ arms expand outward as the pH becomes more acidic or basic. Weisel and Medved [45] used microcalorimetry and electron microscopy to show that under neutral pH, αC domains interact with the E domain; however, under acidic conditions, these interactions are dissociated and αC domains stretch outward.

4.3. Effect of pH on Protein Size

Proteins unfolding as the pH is adjusted may cause considerable changes in their sizes. The effects of pH on HSA and fibrinogen size are discussed below.

4.3.1. Effect of pH Albumin Size

In a study to observe the effect of pH on the globule size of HSA, Luik et al. [46] reported that HSA has its most compacted size, or, more specifically, its lowest Stokes diameter, at physiological pH (7.4). HSA size increases as the pH is increased or decreased. For instance, at an HSA concentration of 2% (w/v), the Stokes diameters at pH values of 5.4, 6.4, 7.4, and 8.0 were around 74 Å, 68 Å, 62 Å, and 72 Å, respectively. Similarly, Reichenwallner et al. [40] determined albumin hydrodynamic radii at various pH values using dynamic light scattering (DLS). They determined that albumin assumes a compact form around neutral pH, but it exhibits an extended form when the pH is raised or lowered; for example, in the study, at the pH values of 2, 7, and 12, albumin hydrodynamic radii were ~4.3 nm, ~3.3 nm, and 4.7 nm, respectively.

4.3.2. Effect of pH on Fibrinogen Size

Fibrinogen is described as an elongated structure which could be approximated as a cylinder or prolate spheroid with the dimensions (crystalline state) of $48.7 \text{ nm} \times 3.32 \text{ nm}$ or $48.7 \text{ nm} \times 4.1 \text{ nm}$, respectively [36]. Other modeled structures such as rigid connected squares and rigid linear chains have been proposed by Hyltegren et al. [47].

Wasilewska et al. [35] used hydrodynamic measurement to determine the effect of pH on the effective length of fibrinogen. They found that around the physiological pH, fibrinogen's effective length was 53–55 nm as it assumed a compact conformation. However, at a pH value >4 or >9 , the fibrinogen molecule expanded, likely due to stretching of the αC domains; thus, the effective length increased to 65–68 nm. The authors pointed out that these values are slightly larger than the often-reported length of 47.5 nm from crystallography, a fact that suggests that fibrinogen undergoes a degree of unfolding when in solution.

4.4. Effect of pH on Protein Hydrophobicity

Protein hydrophobicity affects its interaction with other proteins and its propensity to adhere to various surfaces. The effects of pH on HSA and fibrinogen hydrophobicity are discussed below.

4.4.1. Effect of pH on Albumin Hydrophobicity

Overall protein hydrophobicity (buried and exposed regions) is often termed as the degree of hydrophobicity, whereas when only the exposed regions are of interest, it is called the average surface hydrophobicity [48]. Albumin surface hydrophobicity is affected by the pH in that as it unfolds, more of its internal hydrophobic regions are exposed. Garro et al. [49] studied the effect of pH on HSA by measuring its adsorption of paclitaxel, which is a highly hydrophobic active pharmaceutical ingredient, using a turbidimetry. They found that more paclitaxel was adsorbed at pH of 2.7 and 10 than at pH of 7. For example, at a paclitaxel: HSA molar ratio of 2:1, the optical densities at 600 nm at pH values of 2.7, 7, and 10 were 0.664, 1.386, and 0.694, respectively. The authors hypothesized that the unfolding experienced by HSA at acidic and basic pH exposes additional hydrophobic residues of HSA. As a result, the interaction between HSA and paclitaxel was enhanced, forming a complex that was more soluble, which explained the decrease in optical density.

4.4.2. Effect of pH on Fibrinogen Hydrophobicity

Hydrophobic studies have revealed that the E and D domains of fibrinogen have higher hydrophobicity than the α C domains [23,50]. As mentioned earlier, at around a neutral pH, the structure of fibrinogen is compacted as the positively charged α C domains tug towards the negatively charged E domain, rendering the hydrophobic interactions with other molecules or surfaces preferred. As the pH becomes considerably acidic or basic, the α C domains stretch away from the E domain due to electrostatic repulsion, making these relatively hydrophilic domains available [20]. It has been proposed that when interacting with a hydrophobic surface, the D domains for fibrinogen attach to the surface. However, when the surface is hydrophilic, the adsorption occurs via the α C domains in either hidden or exposed conformations (i.e., compact or extended conformations) [24].

4.5. Effect of pH on Protein Denaturation

Salt bridges among various oppositely charged groups play a role in a protein maintaining a folded structure. Since these salt bridges are a consequence of the protonation state of these groups, a change in the pH can disrupt them (because pH alters the ionization state of these groups), resulting in a degree of protein unfolding or denaturing [51]. The change in the pH also destabilizes some other hydrogen bonds in a protein structure. The effect of pH on the denaturation of HSA can be observed by determining the fractions of α -helix and β -sheet. Dockal et al. [52] showed that the fraction of α -helix was highest around the physiological pH of 7.4. The α -helix fraction decreased as the pH was increased or decreased away from the physiological value. The β -sheet fraction exhibited the opposite. The authors also examined the changes in the fractions of α -helix and β -sheet in the three domains of HSA. Domains I and III displayed similar trends as the overall HSA (i.e., drop in α -helix fraction and rise in β -sheet fraction); however, Domain II's α -helix fraction marginally changed as the pH became more acidic. Similar results of a loss of α -helix structure as the pH was varied from the physiological value were reported by Wallevik [53] and Usoltsev et al. [54]. Usoltsev et al. [54] asserted that generally, HSA denaturing results in the reduction in the α -helix fraction and an increase in β -sheet and random coil fractions.

Fibrous proteins such as fibrinogen have limited tertiary structures; thus, the effect of pH on the unfolding of their structures is minimal in comparison to that on globular proteins. This may explain the scarcity of literature on the effect of pH on fibrinogen denaturation. At any rate, it has been proposed that fibrinogen unfolding could be due to unravelling of the γ -nodule or of the coiled-coil connectors. Moreover, the extension of the α C domains and their unfolding have been shown to occur during fibrinogen

denaturation [22,55]. In addition, protein conformational fluctuations affect the hydration shell dynamics in a heterogeneous manner across the protein surface.

4.6. Using Bovine Serum Albumin as a Surrogate

The number of studies using bovine serum albumin far exceeds that of human serum albumin primarily because of its comparative affordability [56]. Furthermore, BSA and HSA have comparable binding properties and structure. Hence, BSA is often used as a model compound and a replacement for HSA in many studies [57]. BSA polypeptide contains 583 amino acids (vs. 585 for HSA). The two have a sequence identity of around 75.8% [29]. Table 2 shows the comparison between HSA and BSA.

Table 2. Comparison of HSA vs. BSA (adopted from [12,29,58]).

	HSA	BSA
Hydrodynamic radius	3.3–4.3	3.3–4.1
Charge at pH = 7	−9	−11
Overall hydrophathy	−279.2	−230.8
Isoelectric point	4.6	4.6

Generally, the pH has the same effects on BSA properties as it does on HSA. For instance, using Dynamic Light Scattering (DLS), Kun et al. [59] reported that the hydrodynamic mean diameter of BSA in a 0.5 wt % solution was smallest around a pH of 7 (~5 nm) but increased as the pH was increased or decreased (~12 nm at pH of 10 and ~40 nm at pH of 2). Using microcalorimetric and fluorescence measurement, the authors also showed that BSA undergoes similar conformational changes as HSA, with the N-form occurring around the neutral pH. Similar trends have been reported by Li et al. [60] and Sadler and Tucker [61]. The zeta potential behavior of BSA versus pH exhibits the same relationship as shown above for HSA [60]. The zeta potential values are positive above BSA's isoelectric point of ~4.7 but negative below it. As for BSA hydrophobicity, Li et al. [60] reported that changes in the pH away from neutral pH cause BSA to unfold, thus exposing more hydrophobic groups. The authors used fluorescence intensity measurement, between the pH values of 3 and 7, to determine BSA hydrophobicity. The intensity at ~475 nm increased as the pH decreased, indicating a rise in hydrophobicity. Despite the similarities between BSA and HSA, Maier et al. [29] argued that subtle differences, such as the fact that HSA is more hydrophobic than BSA, may have significant ramifications in terms of the adsorption behavior of each protein.

5. Effect of pH on Human Serum Globulins

Besides albumin and fibrinogen, the bulk of the remaining proteins is collectively known as serum globulins (25–35 g/L) [17]. Serum globulins are categorized into α_1 , α_2 , β , and γ globulins. Serum transferrin, an abundant β -globulin, has been used in adsorption and biocompatibility studies as a representative of serum globulins [17,62,63]. Thus, it is briefly discussed in this review. Transferrin has a concentration of ~2.5 g/L and 30% iron saturation, and its function is iron transport [64]. Its ability to bind iron is pH-sensitive, where iron is efficiently bound in the pH range of 7.5–10 but is released in the pH range of 4.5–6.5. Transferrin assumes open conformation when the pH is acidic; however, it adapts a closed conformation in a neutral to basic environment [65].

Transferrin is a glycoprotein that is made up of a polypeptide chain which has 676 amino acids and a molecular weight of 80 kDa. The polypeptide chain forms two globular lobes (a C-lobe and N-lobe). The two lobes are separated by a short helical spacer [66]. Transferrin's shape has been described as a prolate ellipsoid with an axis ratio of 3:1 for an iron-free molecule (i.e., open form) and 2:1 for an iron-saturated molecule (i.e., closed form) [67]. The human serum transfer isoelectric point is ~5.7 [68], but it may vary slightly due to the presence or absence of iron or sialic acid [69].

The authors of this review observed a lack of literature on serum transferrin as it relates to adsorption and fouling. Similarly, Westphalen et al. [17] pointed out that although the transferrin level in the blood is known to affect the outcome of membrane-related treatment such as dialysis, research is scarce. As mentioned earlier, studies such as those by Mollahosseini et al. [62] and Saadati et al. [63] have shed light on the understanding of the transferrin adsorption mechanism within the membrane and biocompatibility context.

6. Protein Structure Prediction via Software

Protein structure modeling using software has been leveraged to overcome some of the above-mentioned challenges. Two computational modeling routes are generally followed: template-based modeling (TBM) and neural network-based modeling (NN). The interactive threading assembly refinement (I-TASSER) is an example of TBM. Some of the TBM methods have been revamped, e.g., I-TASSER-MTD [70] and I-TASSER-GATEWAY [71], and used to predict the protein structure and function. I-TASSER employs a sequence-to-structure-to-function approach by first using the amino acid sequence to propose a 3D structure, and then, through comparison of the 3D structure of known proteins, a function of the created model is inferred [72].

TBM popularity may be dwindling because its predictive accuracy depends on the availability of resembling templates of the protein to be modeled [73]. Additionally, recent successes of the network-based modeling approaches such as AlphaFold 2 [74] and RoseTTAFold [75] have researchers intrigued [73,74]. A comparative study of Lee et al. (2022) [73] illustrated that TBM methods such as Modeller may outperform AlphaFold 2 and RoseTTAFold when no known templates are available.

AlphaFold 2 is deep learning, artificial intelligence software capable of generating accurate protein 3D structure at a resolution approaching that of the experimental data [76]. It uses protein sequences, structures, and template data, along with evolutionary information and possible spatial constraints of the structure, in the prediction process [74,77]. RoseTTAFold is another deep learning software for protein structure prediction. Though it might not be as accurate as AlphaFold 2 in determining the structure of a single-chain protein, RoseTTAFold can give rapid results and can even predict protein-protein complexes. It is a three-track model in that it concurrently evaluates a protein's sequence, plausible interactions among amino acids, and the overall 3D structure [75]. A recent review by Pearce and Zhang [78] adequately addressed various TBM and NN methods and provided a list of open source links available for predicting protein structure. The list includes over 35 entries.

7. Conclusions

Proteins' physiochemical properties are affected by environmental factors such as pH. Hence, modeling human serum proteins as hard spheres with homogenous characteristics might not give an accurate picture. Looking closely at the effects of pH on protein properties such as charge, size, hydrophobicity, conformation, and denaturation may help in developing better fouling models. Our review, which focused on the effect of pH on HSA and fibrinogen, yielded the following:

- Both HSA and fibrinogen carry a positive charge at lower pH values, a negative charge at higher pH values, and are neutral at their isoelectric points. These changes may affect their electrostatic interactions.
- Both HSA and fibrinogen increase in size (e.g., hydrodynamic radius) as the pH moves away from the physiological value. The unfolding may affect its steric behavior.
- Unfolding of HSA and fibrinogen may increase their surface hydrophobicity, affecting their adsorption and aggregation behavior.
- Because HSA is globular, in comparison to fibrinogen, which is fibrous, it is affected more by changes in pH as it unfolds.

8. Outlook

Protein–protein interactions and protein–surface interactions are affected by the electrostatic, steric, and hydrophobic properties of the protein. These properties change as the pH is altered. Although modeling a protein as a hard sphere may reduce the complexity of the process, it may be ignoring some pertinent phenomena.

As researchers seek to refine fouling models so that they are more reflective of reality, incorporating the transformations experienced by a protein as its environment is changed into a model becomes crucial. It is worth noting that Su et al. [4] quantified the internal fouling thickness of HSA on an alumina membrane at the pH values of 3, 5, and 7; the thicknesses were determined to be ~ 3 Å, 42 Å, and 21 Å, respectively. Following the hard-sphere modeling approach may capture these observations. However, a closer look at pH's effect on the steric, hydrophobic, and electrostatic properties of HSA may offer a better explanation. At pH 3, HSA undergoes a considerable degree of unfolding, leading to a size increase and exposure of more hydrophobic portions, which enhance its aggregation. The net effect is the inability, or limited ability, of the protein and protein aggregates to enter membrane pores. At pH 5, a value close to HSA's isoelectric point, the HSA charge approaches zero and the hydrophobic effect becomes dominant, increasing protein–protein and protein–membrane interactions. Lastly, at pH 7, HSA carries a negative charge, causing significant protein–protein repulsion. To reiterate, capturing such effects in a model may not be possible without deviating from the hard-sphere view. One corrective approach is to develop sub-models that capture the effect of pH on a protein's size, charge, hydrophobicity, etc., and then incorporate them into an overall fouling model. Our ongoing research is currently considering incorporating the critical influence of pH into a fouling model of human serum proteins.

Author Contributions: Conceptualization, A.A.; formal analysis, M.M.; writing—original draft preparation, M.M.; writing—review and editing, A.A.; supervision, A.A.; project administration, A.A.; funding acquisition, A.A. All authors have read and agreed to the published version of the manuscript.

Funding: The authors acknowledge the Natural Sciences and Engineering Research Council of Canada (NSERC) for funding the research and the Chemical and Biological Engineering Department of the University of Saskatchewan for the support provided.

Institutional Review Board Statement: Amira Abdelrasoul, the principal investigator of the project, obtained Research Ethics Approval and Operational Approval to conduct this research in the Saskatchewan Health Authority. She is responsible for regulatory approvals that pertain to this project, and for ensuring the project was conducted according to the governing law.

Data Availability Statement: The information about the data presented in the article is available from the corresponding authors (Amira Abdelrasoul; A.A.) upon reasonable request.

Conflicts of Interest: The authors declare no conflict of interest.

References

1. Uwaezuoke, O.J.; Kumar, P.; Pillay, V.; Choonara, Y.E. Fouling in Ocular Devices: Implications for Drug Delivery, Bioactive Surface Immobilization, and Biomaterial Design. *Drug Deliv. Transl. Res.* **2021**, *11*. [[CrossRef](#)]
2. Finch, C.; Clarke, T.; Hickman, J.J. A Continuum Hard-Sphere Model of Protein Adsorption. *J. Comput. Phys.* **2013**, *244*, 212–222. [[CrossRef](#)]
3. Stradner, A.; Schurtenberger, P. Potential and Limits of a Colloid Approach to Protein Solutions. *Soft Matter* **2020**, *16*, 307–323. [[CrossRef](#)]
4. Su, T.J.; Lu, J.R.; Cui, Z.F.; Thomas, R.K. Fouling of Ceramic Membranes by Albumins under Dynamic Filtration Conditions. *J. Membr. Sci.* **2000**, *173*, 167–178. [[CrossRef](#)]
5. Pasche, S.; Vörös, J.; Griesser, H.J.; Spencer, N.D.; Textor, M. Effects of Ionic Strength and Surface Charge on Protein Adsorption at PEGylated Surfaces. *J. Phys. Chem. B* **2005**, *109*. [[CrossRef](#)]
6. Nattich-Rak, M.; Dąbkowska, M.; Adamczyk, Z. Microparticle Deposition on Human Serum Albumin Layers: Unraveling Anomalous Adsorption Mechanism. *Colloids Interfaces* **2020**, *4*. [[CrossRef](#)]

7. Tsapikouni, T.S.; Missirlis, Y.F. PH and Ionic Strength Effect on Single Fibrinogen Molecule Adsorption on Mica Studied with AFM. *Colloids Surf. B Biointerfaces* **2007**, *57*. [[CrossRef](#)]
8. Pragna Lakshmi, T.; Mondal, M.; Ramadas, K.; Natarajan, S. Molecular Interaction of 2,4-Diacetylphloroglucinol (DAPG) with Human Serum Albumin (HSA): The Spectroscopic, Calorimetric and Computational Investigation. *Spectrochim. Acta A Mol. Biomol. Spectrosc.* **2017**, *183*, 90–102. [[CrossRef](#)]
9. Sen, P.; Khan, M.M.; Eqbal, A.; Ahmad, E.; Khan, R.H. At Very Low Concentrations Known Chaotropes Act as Kosmotropes for the N and B Isoforms of Human Serum Albumin. *Biochem. Cell Biol.* **2013**, *91*, 72–78. [[CrossRef](#)]
10. Parodi, A.; Miao, J.; Soond, S.M.; Rudzińska, M.; Zamyatnin, A.A. Albumin Nanovectors in Cancer Therapy and Imaging. *Biomolecules* **2019**, *9*. [[CrossRef](#)] [[PubMed](#)]
11. Ekowati, R.; B, S.S.; W, S.D. Molecular Dynamics Simulation for Revealing the Role of Water Molecules on Conformational Change of Human Serum Albumin. *Int. J. Pharm. Clin. Res.* **2016**, *8*, 158–161.
12. Akdogan, Y.; Reichenwallner, J.; Hinderberger, D. Evidence for Water-Tuned Structural Differences in Proteins: An Approach Emphasizing Variations in Local Hydrophilicity. *PLoS ONE* **2012**, *7*. [[CrossRef](#)] [[PubMed](#)]
13. Abou-Zied, O.K.; Al-Lawatia, N. Exploring the Drug-Binding Site Sudlow I of Human Serum Albumin: The Role of Water and Trp214 in Molecular Recognition and Ligand Binding. *Chemphyschem* **2011**, *12*, 270–274. [[CrossRef](#)] [[PubMed](#)]
14. Rothschild, M.A.; Oratz, M.; Schreiber, S.S. Serum Albumin. *Hepatology* **1988**, *8*, 385–401. [[CrossRef](#)] [[PubMed](#)]
15. Horbett, T.A. Fibrinogen Adsorption to Biomaterials. *J. Biomed. Mater. Res. Part A* **2018**, *106*, 2777–2788. [[CrossRef](#)] [[PubMed](#)]
16. Labarrere, C.A.; Dabiri, A.E.; Kassab, G.S. Thrombogenic and Inflammatory Reactions to Biomaterials in Medical Devices. *Front. Bioeng. Biotechnol.* **2020**, *8*. [[CrossRef](#)]
17. Westphalen, H.; Kalugin, D.; Abdelrasoul, A. Structure, Function, and Adsorption of Highly Abundant Blood Proteins and Its Critical Influence on Hemodialysis Patients: A Critical Review. *Biomed. Eng. Adv.* **2021**, *2*, 100021. [[CrossRef](#)]
18. Mosesson, M.W. Fibrinogen and Fibrin Structure and Functions. *J. Thromb. Haemost.* **2005**, *3*, 1894–1904. [[CrossRef](#)]
19. Weisel, J.W.; Litvinov, R.I. Fibrin Formation, Structure and Properties. *Subcell. Biochem.* **2017**, *82*, 405–456. [[CrossRef](#)]
20. Hu, Y.; Jin, J.; Liang, H.; Ji, X.; Yin, J.; Jiang, W. PH Dependence of Adsorbed Fibrinogen Conformation and Its Effect on Platelet Adhesion. *Langmuir* **2016**, *32*, 4086–4094. [[CrossRef](#)]
21. Tiscia, G.L.; Margaglione, M. Human Fibrinogen: Molecular and Genetic Aspects of Congenital Disorders. *Int. J. Mol. Sci.* **2018**, *19*. [[CrossRef](#)]
22. Zhmurov, A.; Brown, A.E.X.; Litvinov, R.I.; Dima, R.I.; Weisel, J.W.; Barsegov, V. Mechanism of Fibrin(Ogen) Forced Unfolding. *Structure* **2011**, *19*, 1615–1624. [[CrossRef](#)] [[PubMed](#)]
23. van de Keere, I.; Willaert, R.; Hubin, A.; Vereecken, J. Interaction of Human Plasma Fibrinogen with Commercially Pure Titanium as Studied with Atomic Force Microscopy and X-Ray Photoelectron Spectroscopy. *Langmuir* **2008**, *24*, 1844–1852. [[CrossRef](#)] [[PubMed](#)]
24. Stamboroski, S.; Joshi, A.; Michael Noeske, P.-L.; Köppen, S.; Brüggemann, D.; Stamboroski, S.; Noeske, P.M.; Joshi, A.; Brüggemann, D. Principles of Fibrinogen Fiber Assembly In Vitro. *Macromol. Biosci.* **2021**, *21*, 2000412. [[CrossRef](#)] [[PubMed](#)]
25. Dumetz, A.C.; Chockla, A.M.; Kaler, E.W.; Lenhoff, A.M. Effects of PH on Protein-Protein Interactions and Implications for Protein Phase Behavior. *Biochim. Biophys. Acta Proteins Proteom.* **2008**, *1784*. [[CrossRef](#)] [[PubMed](#)]
26. Lošdorfer Božič, A.; Podgornik, R. PH Dependence of Charge Multipole Moments in Proteins. *Biophys. J.* **2017**, *113*, 1454–1465. [[CrossRef](#)]
27. Belinskaia, D.A.; Voronina, P.A.; Shmurak, V.I.; Jenkins, R.O.; Goncharov, N.V. Serum Albumin in Health and Disease: Esterase, Antioxidant, Transporting and Signaling Properties. *Int. J. Mol. Sci.* **2021**, *22*. [[CrossRef](#)]
28. Hierro-Oliva, M.; Gallardo-Moreno, A.M.; González-Martín, M.L. Surface Characterisation of Human Serum Albumin Layers on Activated Ti6Al4V. *Materials* **2021**, *14*. [[CrossRef](#)]
29. Maier, R.; Fries, M.R.; Buchholz, C.; Zhang, F.; Schreiber, F. Human versus Bovine Serum Albumin: A Subtle Difference in Hydrophobicity Leads to Large Differences in Bulk and Interface Behavior. *Cryst. Growth Des.* **2021**, *21*, 5451–5459. [[CrossRef](#)]
30. Fogh-Andersen, N.; Bjerrum, P.J.; Siggaard-Andersen, O. Ionic Binding, Net Charge, and Donnan Effect of Human Serum Albumin as a Function of PH. *Clin. Chem.* **1993**, *39*. [[CrossRef](#)]
31. Peters, T. *All about Albumin: Biochemistry, Genetics, and Medical Applications*; Academic Press: Cambridge, MA, USA, 1995.
32. Sze, A.; Erickson, D.; Ren, L.; Li, D. Zeta-Potential Measurement Using the Smoluchowski Equation and the Slope of the Current–Time Relationship in Electroosmotic Flow. *J. Colloid Interface Sci.* **2003**, *261*, 402–410. [[CrossRef](#)] [[PubMed](#)]
33. O’connor, A.J.; Pratt, H.R.C.; Stevens, G.W. Electrophoretic mobilities of proteins and protein mixtures in porous membranes. *Chem. Eng. Sci.* **1996**, *51*, 3459–3477. [[CrossRef](#)]
34. Jun, B.M.; Cho, J.; Jang, A.; Chon, K.; Westerhoff, P.; Yoon, Y.; Rho, H. Charge Characteristics (Surface Charge vs. Zeta Potential) of Membrane Surfaces to Assess the Salt Rejection Behavior of Nanofiltration Membranes. *Sep. Purif. Technol.* **2020**, *247*. [[CrossRef](#)]
35. Wasilewska, M.; Adamczyk, Z.; Jachimska, B. Structure of Fibrinogen in Electrolyte Solutions Derived from Dynamic Light Scattering (DLS) and Viscosity Measurements. *Langmuir* **2009**, *25*, 3698–3704. [[CrossRef](#)]
36. Adamczyk, Z.; Wasilewska, M.; Nattich-Rak, M.; Barbasz, J.; Haber, J. Mechanisms of Fibrinogen Adsorption on Mica. *ACS Symp. Ser.* **2012**, *1120*, 97–127.
37. Kusova, A.M.; Sitnitsky, A.E.; Zuev, Y.F. The Role of PH and Ionic Strength in the Attraction-Repulsion Balance of Fibrinogen Interactions. *Langmuir* **2021**, *37*, 10394–10401. [[CrossRef](#)] [[PubMed](#)]

38. Wasilewska, M.; Adamczyk, Z. Fibrinogen Adsorption on Mica Studied by AFM and in Situ Streaming Potential Measurements. *Langmuir* **2011**, *27*, 686–696. [[CrossRef](#)] [[PubMed](#)]
39. Qiu, W.; Zhang, L.; Okobiah, O.; Yang, Y.; Wang, L.; Zhong, D.; Zewail, A.H. Ultrafast Solvation Dynamics of Human Serum Albumin: Correlations with Conformational Transitions and Site-Selected Recognition. *J. Phys. Chem. B* **2006**, *110*, 10540–10549. [[CrossRef](#)] [[PubMed](#)]
40. Reichenwallner, J.; Oehmichen, M.T.; Schmelzer, C.E.H.; Hauenschild, T.; Kerth, A.; Hinderberger, D. Exploring the Ph-Induced Functional Phase Space of Human Serum Albumin by Epr Spectroscopy. *Magnetochemistry* **2018**, *4*. [[CrossRef](#)]
41. Baler, K.; Martin, O.A.; Carignano, M.A.; Ameer, G.A.; Vila, J.A.; Szleifer, I. Electrostatic Unfolding and Interactions of Albumin Driven by PH Changes: A Molecular Dynamics Study. *J. Phys. Chem. B* **2014**, *118*, 921–930. [[CrossRef](#)]
42. Carter, D.C.; Ho, J.X. Structure of Serum Albumin. *Adv. Protein Chem.* **1994**, *45*, 153–176. [[CrossRef](#)] [[PubMed](#)]
43. Sønderby, P.; Bukrinski, J.T.; Hebditch, M.; Peters, G.H.J.; Curtis, R.A.; Harris, P. Self-Interaction of Human Serum Albumin: A Formulation Perspective. *ACS Omega* **2018**, *3*. [[CrossRef](#)] [[PubMed](#)]
44. Wu, H.; Zhang, R.; Zhang, W.; Hong, J.; Xiang, Y.; Xu, W. Rapid 3-Dimensional Shape Determination of Globular Proteins by Mobility Capillary Electrophoresis and Native Mass Spectrometry. *Chem. Sci.* **2020**, *11*, 4758–4765. [[CrossRef](#)]
45. Weisel, J.W.; Medved, L. The Structure and Function of the AC Domains of Fibrinogen. *Ann. N. Y. Acad. Sci.* **2001**, *936*, 312–327. [[CrossRef](#)]
46. Luik, A.I.; Naboka, Y.N.; Mogilevich, S.E.; Hushcha, T.O.; Mischenko, N.I. Study of Human Serum Albumin Structure by Dynamic Light Scattering: Two Types of Reactions under Different PH and Interaction with Physiologically Active Compounds. *Spectrochim. Acta A Mol. Biomol. Spectrosc.* **1998**, *54*, 1503–1507. [[CrossRef](#)] [[PubMed](#)]
47. Hyltegren, K.; Hulander, M.; Andersson, M.; Skepö, M. Adsorption of Fibrinogen on Silica Surfaces—The Effect of Attached Nanoparticles. *Biomolecules* **2020**, *10*. [[CrossRef](#)] [[PubMed](#)]
48. Lienqueo, M.E.; Mahn, A.; Salgado, J.C.; Asenjo, J.A. Current Insights on Protein Behaviour in Hydrophobic Interaction Chromatography. *J. Chromatogr. B* **2007**, *849*, 53–68. [[CrossRef](#)]
49. Garro, A.G.; Beltramo, D.M.; Alasino, R.V.; Leonhard, V.; Heredia, V.; Bianco, I.D. Reversible Exposure of Hydrophobic Residues on Albumin as a Novel Strategy for Formulation of Nanodelivery Vehicles for Taxanes. *Int. J. Nanomed.* **2011**, *6*, 1193–1200. [[CrossRef](#)]
50. Horbett, T.A.; Brash, J.L. Proteins at Interfaces II. *ACS Symp. Ser.* **1995**. [[CrossRef](#)]
51. Westphalen, H.; Abdelrasoul, A.; Shoker, A. Protein adsorption phenomena in hemodialysis membranes: Mechanisms, influences of clinical practices, modeling, and challenges. *Colloids Interface Sci. Commun.* **2021**, *40*, 100348. [[CrossRef](#)]
52. Dockal, M.; Carter, D.C.; Rü, F. The Three Recombinant Domains of Human Serum Albumin STRUCTURAL CHARACTERIZATION AND LIGAND BINDING PROPERTIES*. *J. Biol. Chem.* **1999**, *274*, 29303–29310. [[CrossRef](#)] [[PubMed](#)]
53. Wallevik, X. Reversible Denaturation of Human Serum Albumin by PH, Temperature, and Guanidine Hydrochloride Followed by Optical Rotation. *J. Biol. Chem.* **1973**, *248*, 2650–2655. [[CrossRef](#)]
54. Usoltsev, D.; Sitnikova, V.; Kajava, A.; Uspenskaya, M. Systematic FTIR Spectroscopy Study of the Secondary Structure Changes in Human Serum Albumin under Various Denaturation Conditions. *Biomolecules* **2019**, *9*. [[CrossRef](#)] [[PubMed](#)]
55. Guthold, M.; Cho, S.S. Fibrinogen Unfolding Mechanisms Are Not Too Much of a Stretch. *Structure* **2011**, *19*. [[CrossRef](#)] [[PubMed](#)]
56. Mishra, V.; Heath, R.J. Structural and Biochemical Features of Human Serum Albumin Essential for Eukaryotic Cell Culture. *Int. J. Mol. Sci.* **2021**, *22*. [[CrossRef](#)]
57. Rubio-Pereda, P.; Vilhena, J.G.; Takeuchi, N.; Serena, P.A.; Pérez, R. Albumin (BSA) Adsorption onto Graphite Stepped Surfaces. *J. Chem. Phys.* **2017**, *146*. [[CrossRef](#)]
58. Jachimska, B.; Wasilewska, M.; Adamczyk, Z. Characterization of Globular Protein Solutions by Dynamic Light Scattering, Electrophoretic Mobility, and Viscosity Measurements. *Langmuir* **2008**, *24*. [[CrossRef](#)]
59. Kun, R.; Szekeres, M.; Dékány, I. Isothermal Titration Calorimetric Studies of the PH Induced Conformational Changes of Bovine Serum Albumin. *J. Therm. Anal. Calorim.* **2009**, *96*, 1009–1017. [[CrossRef](#)]
60. Li, R.; Wu, Z.; Wang, Y.; Ding, L.; Wang, Y. Role of PH-Induced Structural Change in Protein Aggregation in Foam Fractionation of Bovine Serum Albumin. *Biotechnol. Rep.* **2016**, *9*, 46–52. [[CrossRef](#)]
61. Sadler, P.J.; Tucker, A. PH-induced Structural Transitions of Bovine Serum Albumin: Histidine PKa Values and Unfolding of the N-terminus during the N to F Transition. *Eur. J. Biochem.* **1993**, *212*. [[CrossRef](#)]
62. Mollahosseini, A.; Saadati, S.; Abdelrasoul, A. A Comparative Assessment of Human Serum Proteins Interactions with Hemodialysis Clinical Membranes Using Molecular Dynamics Simulation. *Macromol. Theory Simul.* **2022**, *31*, 2200016. [[CrossRef](#)]
63. Saadati, S.; Eduok, U.; Westphalen, H.; Abdelrasoul, A.; Shoker, A.; Choi, P.; Doan, H.; Ein-Mozaffari, F.; Zhu, N. Assessment of Polyethersulfone and Polyacrylonitrile Hemodialysis Clinical Membranes: In Situ Synchrotron-Based Imaging of Human Serum Proteins Adsorption, Interaction Analyses, Molecular Docking and Clinical Inflammatory Biomarkers Investigations. *Mater. Today Commun.* **2021**, *29*. [[CrossRef](#)]
64. Silva, A.M.N.; Moniz, T.; de Castro, B.; Rangel, M. Human Transferrin: An Inorganic Biochemistry Perspective. *Coord. Chem. Rev.* **2021**, *449*, 214186. [[CrossRef](#)]
65. Mazurier, J.; Spik, G. Comparative Study of the Iron-Binding Properties of Human Transferrins. I. Complete and Sequential Iron Saturation and Desaturation of the Lactotransferrin. *Biochim. Biophys. Acta* **1980**, *629*, 399–408. [[CrossRef](#)]

66. Gomme, P.T.; McCann, K.B.; Bertolini, J. Transferrin: Structure, Function and Potential Therapeutic Actions. *Drug Discov. Today* **2005**, *10*. [[CrossRef](#)]
67. Welch, S. *Transferrin: The Iron Carrier*; CRC Press: Cleveland, OH, USA, 1992; p. 304.
68. Vesterberg, O.; Breig, U. Quantitative Analysis of Multiple Molecular Forms of Transferrin Using Isoelectric Focusing and Zone Immunoelectrophoresis Assay (ZIA). *J. Immunol. Methods* **1981**, *46*. [[CrossRef](#)]
69. Marquardt, T.; Denecke, J. Congenital Disorders of Glycosylation: Review of Their Molecular Bases, Clinical Presentations and Specific Therapies. *Eur. J. Pediatr.* **2003**, *162*. [[CrossRef](#)]
70. Zhou, X.; Zheng, W.; Li, Y.; Pearce, R.; Zhang, C.; Bell, E.W.; Zhang, G.; Zhang, Y. I-TASSER-MTD: A Deep-Learning-Based Platform for Multi-Domain Protein Structure and Function Prediction. *Nat. Protoc.* **2022**, *17*, 2326–2353. [[CrossRef](#)]
71. Zheng, W.; Zhang, C.; Bell, E.W.; Zhang, Y. I-TASSER Gateway: A Protein Structure and Function Prediction Server Powered by XSEDE. *Future Gener. Comput. Syst.* **2019**, *99*. [[CrossRef](#)]
72. Roy, A.; Kucukural, A.; Zhang, Y. I-TASSER: A Unified Platform for Automated Protein Structure and Function Prediction. *Nat Protoc* **2010**, *5*. [[CrossRef](#)]
73. Lee, C.; Su, B.-H.; Jane Tseng Corresponding author Tseng, Y.Y. Comparative Studies of AlphaFold, RoseTTAFold and Modeller: A Case Study Involving the Use of G-Protein-Coupled Receptors. *Brief Bioinform.* **2022**, *23*, 1–7. [[CrossRef](#)]
74. Jumper, J.; Evans, R.; Pritzel, A.; Green, T.; Figurnov, M.; Ronneberger, O.; Tunyasuvunakool, K.; Bates, R.; Židek, A.; Potapenko, A.; et al. Highly Accurate Protein Structure Prediction with AlphaFold. *Nature* **2021**, *596*. [[CrossRef](#)]
75. Baek, M.; DiMaio, F.; Anishchenko, I.; Dauparas, J.; Ovchinnikov, S.; Lee, G.R.; Wang, J.; Cong, Q.; Kinch, L.N.; Dustin Schaeffer, R.; et al. Accurate Prediction of Protein Structures and Interactions Using a Three-Track Neural Network. *Science* **2021**, *373*. [[CrossRef](#)]
76. Skolnick, J.; Gao, M.; Zhou, H.; Singh, S. AlphaFold 2: Why It Works and Its Implications for Understanding the Relationships of Protein Sequence, Structure, and Function. *J. Chem. Inf. Model.* **2021**, *61*. [[CrossRef](#)]
77. Goulet, A.; Cambillau, C. Present Impact of AlphaFold2 Revolution on Structural Biology, and an Illustration with the Structure Prediction of the Bacteriophage J-1 Host Adhesion Device. *Front. Mol. Biosci.* **2022**, *9*, 1–7. [[CrossRef](#)]
78. Pearce, R.; Zhang, Y. Toward the Solution of the Protein Structure Prediction Problem. *J. Biol. Chem.* **2021**, *297*. [[CrossRef](#)]

Disclaimer/Publisher's Note: The statements, opinions and data contained in all publications are solely those of the individual author(s) and contributor(s) and not of MDPI and/or the editor(s). MDPI and/or the editor(s) disclaim responsibility for any injury to people or property resulting from any ideas, methods, instructions or products referred to in the content.